

PAPER • OPEN ACCESS

Photo-irradiation induced green synthesis of highly stable silver nanoparticles using durian rind biomass: effects of light intensity, exposure time and pH on silver nanoparticles formation

To cite this article: Fueangfahkan Chutrakulwong *et al* 2020 *J. Phys. Commun.* 4 095015

View the [article online](#) for updates and enhancements.



PAPER

OPEN ACCESS

RECEIVED
21 July 2020REVISED
26 August 2020ACCEPTED FOR PUBLICATION
2 September 2020PUBLISHED
14 September 2020

Original content from this work may be used under the terms of the [Creative Commons Attribution 4.0 licence](#).

Any further distribution of this work must maintain attribution to the author(s) and the title of the work, journal citation and DOI.



Photo-irradiation induced green synthesis of highly stable silver nanoparticles using durian rind biomass: effects of light intensity, exposure time and pH on silver nanoparticles formation

Fueangfahkan Chutrakulwong¹ , Kheamrutai Thamaphat¹ and Pichet Limsuwan²¹ Green Synthesis and Application Laboratory, Applied Science and Engineering for Social Solution Research Unit, Department of Physics, Faculty of Science, King Mongkut's University of Technology Thonburi, Bangkok 10140, Thailand² Applied Optics and Laser Research Laboratory, Department of Physics, Faculty of Science, King Mongkut's University of Technology Thonburi, Bangkok 10140, ThailandE-mail: kheamrutai.tha@kmutt.ac.th

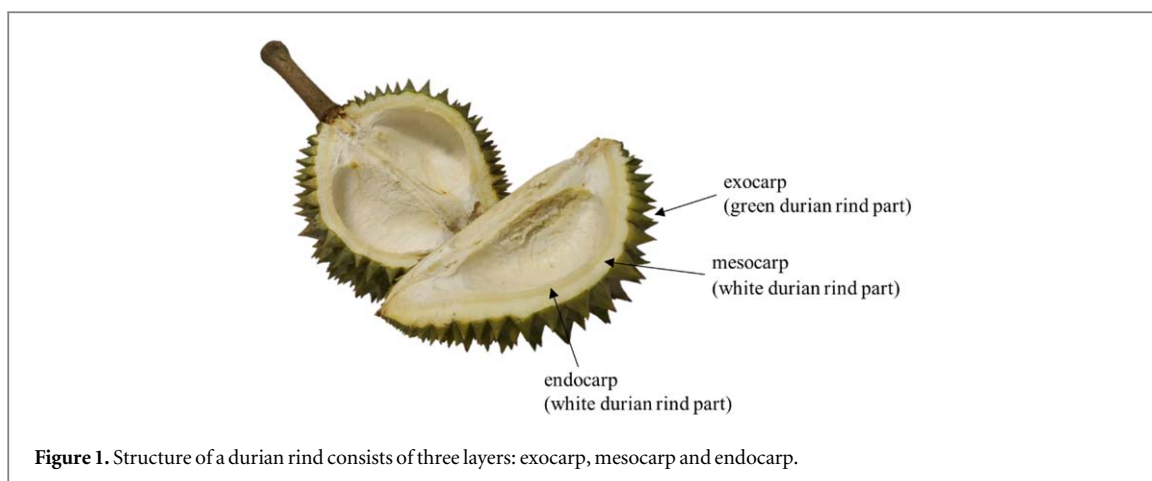
Keywords: silver nanoparticle, durian rind, photoreduction, green synthesis

Abstract

The purpose of this work is to single-pot biosynthesize silver nanoparticles (AgNPs) using the extract from mesocarp and endocarp of durian rind under photo-irradiation. Without adding chemical substance, flavonoids, phenolic compounds and glucose dissolved in the extract served as the reducing agent; while proteins acted as the particle-stabilizing agent in the formation of AgNPs. The synthesis parameters i.e. light intensity, exposure duration, and pH value directly associated with the nucleation, growth, and aggregation of nanoparticles. The amount of synthesized AgNPs increased with increasing visible light intensity and exposure duration, while the size and stability of nanoparticles were decided by pH value adjustment. The size of synthesized AgNPs decreased when the pH value increased, on the contrary, the size increased when the pH value decreased. Under the optimized synthesis conditions (visible light intensity of 13,430 lx and pH value of 8.5), approximately 99% of silver ions was reduced to the spherical AgNPs with the mean diameter of 11.4 ± 3.2 nm within 5 min. The AgNPs remained uniformly dispersed in de-ionized water at no less than six months. The present environmental-friendly method is facile, rapid, and cost effective for the large scale preparation of AgNPs. The obtained AgNPs synthesized under optimum conditions could be applied for use in various fields such as antimicrobial activity, biosensors, and catalysis in the near future.

1. Introduction

Silver nanoparticles (AgNPs) are considered as one of the most attractive metallic nanomaterials owing to their wide range of applications with excellent performance such as antimicrobials [1, 2], catalysis [3], chemical and bimolecular detections [4, 5], and Raman scattering enhancement [6]. These unique nanoscale activities of AgNPs sensitivity depend on size, shape, surface coating, and surface chemistry of nanostructured materials. Consequently, many efforts have been currently emphasized on exploring synthetic routes that enable to control size, shape, distribution, and monodispersity of the synthesized AgNPs [7–9]. Among several reported synthetic methods of AgNPs, the most common methods rely on a chemical reduction of silver ions (Ag^+) dissolved in silver salt solutions into silver atoms (Ag^0) using strong chemical reducing agents, such as sodium borohydride, sodium citrate, ascorbate, etc, in different stabilizing agents to prevent particles agglomeration [10, 11]. In addition, the sonication [12, 13], microwave radiation [14] and photoreduction [15–17] have been employed to assist the chemical reaction for improvement in homogeneous nucleation and growth of AgNPs. However, many methods involve high energy requirement and toxic chemicals, which are potentially harmful to environment, ecosystem, and human health. To step over these problems, the emergence of environment-friendly green chemistry is therefore applied for biosynthesis of metal nanoparticles particularly AgNPs. A number of natural substance, enzyme, microorganism, leaf extract, latex extract, seed extract, fruit extract,



nutritious food and so on have shown success in the synthesis of AgNPs [2, 18–27]. Nevertheless, several bioextracts require other purification technique, complicated preparation process, long reaction time, and high thermal energy. In this sense, the development of a novel and very economical green route for synthesis of well stabilized and size-controlled AgNPs is still addressed as one of the main challenges in the current researches.

Durian (*Durio zibethinus* Murr.; family *Bombacaceae*, genus *Durio*) regarded as the ‘king of fruits’ is one of the most important tropical fruit of Thailand including Southeast Asia countries such as Malaysia, Indonesia, Philippines following by Singapore. Currently, Thailand is the world’s largest exporter of fresh and frozen durian approximately 500,000 tons in the year 2019, according to the Office of Agricultural Economics (OAE - Thailand) [28]. Unexpectedly, the edible portion of durian fruit product accounts only 22%–30% of the mass of the entire fruit, whereas the non-edible parts evaluated the rind and seed residues contribute about 70% depending on their varieties [29]. The durian residues, especially the massive amounts of waste in the form of rind, generated from local markets and manufacturing industries are mostly burned or probably sent to the landfills causing a several problems in the community. Therefore, there need to further explore the optimum procedures for utilization of durian rind. As far as we know, the durian rind contains a high amount of water-insoluble and water-soluble polysaccharides, which are long chains of carbohydrate molecules consisting mainly of D-galacturonic acid and neutral sugars such as L-rhamnose, L-arabinose, D-galactose, D-glucose and D-fructose, and a potential source of natural antioxidants especially polyphenols and flavonoids [30–34]. These biological components promote conversion of Ag + to neutral silver atoms and also simultaneously contribute to stabilize the growth of AgNPs [3, 22, 25, 35–40], as reported in our previous preliminary results [41].

From an elaborate literature review, the utilization of agro-industrial waste mediated synthesis of AgNPs is rarely found; banana peels, citrus peels, and grape stalks were discovered [42–44]. However, only recently, a researcher group has attempted to utilize aqueous extract of durian rind in green synthesis of AgNPs under solar radiation [45]. Unfortunately, the Sunlight intensity is difficult to control, hence, it is a practical problematic point to resynthesize the AgNPs that dominate the same physical, optical and antibacterial properties. Up-to-date, there is no published work on the study of visible light as a catalyst for green synthesis of AgNPs in the presence of durian rind extract. Thus, this present research was a continuation of our previous work with emphasis on the effects of light intensity, exposure time, and pH on the shape, size, yield and stability of AgNPs, and the possible photo-irradiation biosynthesis mechanism was also described.

2. Materials and methods

2.1. Collection of waste material

In the investigation, the Mon Thong durian rind wastes were obtained from an agro-food processing industry located in Chanthaburi province, Thailand for using throughout this work. A large amount of fresh durian rind was washed for several times to remove all contaminant and air dried in shade. As shown in figure 1, the durian rind has three layers: the exocarp or outermost layer, the mesocarp or intermediate layer, and the endocarp or innermost layer [46]. The exocarp can easily be identified by green to brown part covered by hard and sharp thorns. Whereas, the mesocarp is identified as a thick white layer and the endocarp is a very thin white layer located next to the mesocarp. In this work, the exocarp was sliced off, the mesocarp and endocarp (white durian rind part) were collected. They were cut into small pieces, milled to coarse powders with a mechanical grinder, and kept in an air tight plastic container at -20°C until further use. In addition, the durian rind powders were randomly selected to analyze carbohydrate and protein contents according to the Association of Official

Agricultural Chemists (AOAC) Method 922.02, 925.05, and 991.20 [47] using an Agilent 1200 high performance liquid chromatography (HPLC) by the National Food Institute, Thailand.

2.2. Preparation of durian rind extract

The durian rind extract was carried out in batch according to the procedure of bioactive compound extraction. The durian rind powders were subjected to de-ionized water (solid-liquid ratio; 1:5 w/v) in an ultrasound water bath at 60 °C for 30 min. The extract (liquid solution) was separated from solid by filtration through Whatman filter paper No.5 and centrifuged at 6,000 rpm for 15 min. Then, the extract was stored in dark place at 4 °C until use.

2.3. Synthesis of silver nanoparticles

For all experiments, the source of Ag^+ was silver nitrate (AgNO_3) of analytical grade obtained from POCH and the concentration of AgNO_3 solution was kept constant at 1 mM. The synthesis procedure for AgNPs using durian rind extract under photo-irradiation began with adding the extract into 1 mM AgNO_3 solution in the ratio of 1:1. Afterward, the pH of mixture was changed by dropwise addition of 0.1 M hydrochloric acid (Ajax) and 0.1 M sodium hydroxide (Ajax) to achieve the desired value. The 60 ml of resulting mixture was then contained in a 100-ml beaker for investigation of the visible light-mediated straightforward green synthesis of AgNPs. The photo-irradiation was carried out using a 20 W compact fluorescent light bulb with dimmable placed above the reaction container at 20 cm height. The irradiation light intensity was measured at a center position of the reaction container using an Extech LT300 digital light meter. The mixture was irradiated and stirred at 390 rpm inside an assembled exposure box in order to eliminate the interference from surrounding light. The mixture temperature was maintained at 25 ± 1 °C throughout the AgNPs growth process. The effects of light intensity (2,810, 8,120 and 13,430 lx), pH of the solution (6.5, 7.5, 8.5 and 12.0), and exposure time (5 min, 10 min, 30 min, 1 h, 2 h, 3 h, 6 h, 9 h and 12 h) on AgNPs synthesis were investigated. As a control experiment for comparison, the mixture was stirred in a dark place. The as-prepared AgNPs obtained from all experiments were collected to characterize their optical and physical properties.

2.4. Characterization of durian rind extract and silver nanoparticles

The UV-vis absorption spectra of the colloidal solution of AgNPs were recorded in the wavelength range of 300–800 nm using an AvaSpec-2048 Fiber Optic Spectrometer. A JEOL-2100 transmission electron microscope (TEM) operated at 200 kV was used to investigate the size and morphology of the synthesized AgNPs placing on formvar-carbon coated copper grid by drop-coating method. To determine the crystal structure of AgNPs, the centrifuged AgNPs were freeze-dried and transferred to analyze by a Bruker D8 Advance powder x-ray diffraction (XRD) system operated at a voltage of 40 kV and a current of 40 mA using monochromatic $\text{CuK}\alpha$ radiation ($\lambda = 1.5406$ Å). Additionally, the elemental composition was acquired using an energy dispersive x-ray spectroscopy (EDX) with Zeiss LEO 1550VP.

The percent yield for the synthesis reaction was revealed using an inductively coupled plasma-atomic emission spectroscopy (ICP-OES). For sample preparation, the colloidal solution of AgNPs were centrifuged at 14,000 rpm for 10 min, and the silver ion concentration dissolved in the supernatant was then determined using a Perkin-Elmer Optima 3000 system. CertiPUR[®] ICP Ag standard solutions of 1000 mg l^{-1} (Merck, Darmstadt, Germany) were used as stock solution for calibration. In considering, the concentration of silver ion dissolved in solution was obtained from the intensity of Ag I emission line at the wavelength of 328.068 nm. The percent yield of AgNPs synthesis was calculated from a comparison of the residual silver ion concentration with the initial silver ion concentration using the following equation:

$$\% \text{ yield} = \frac{(C_0 - C_r)}{C_0} \times 100\%, \quad (1)$$

where C_0 is the initial silver ion concentration (ppm) and C_r is the residual silver ion concentration (ppm).

Zetasizer (Malver, Nano ZS) instrument was employed to analyze the average size, surface charge, and stability of the AgNPs obtained from the optimum condition. Fourier transform infrared spectroscopy (FTIR) was carried out in order to determine the functional groups present in the durian peel extract and around the AgNPs for understanding the possible mechanism involving the synthesis of AgNPs. The FTIR spectra were recorded at a resolution of 4 cm^{-1} in the range of $4000\text{--}400 \text{ cm}^{-1}$ using a PerkinElmer Spectrum 400 FTIR spectrophotometer.

2.5. Statistical analysis

All experiments were performed in triplicate. The representative results were expressed as the mean \pm standard deviation carried out using the Excel software.

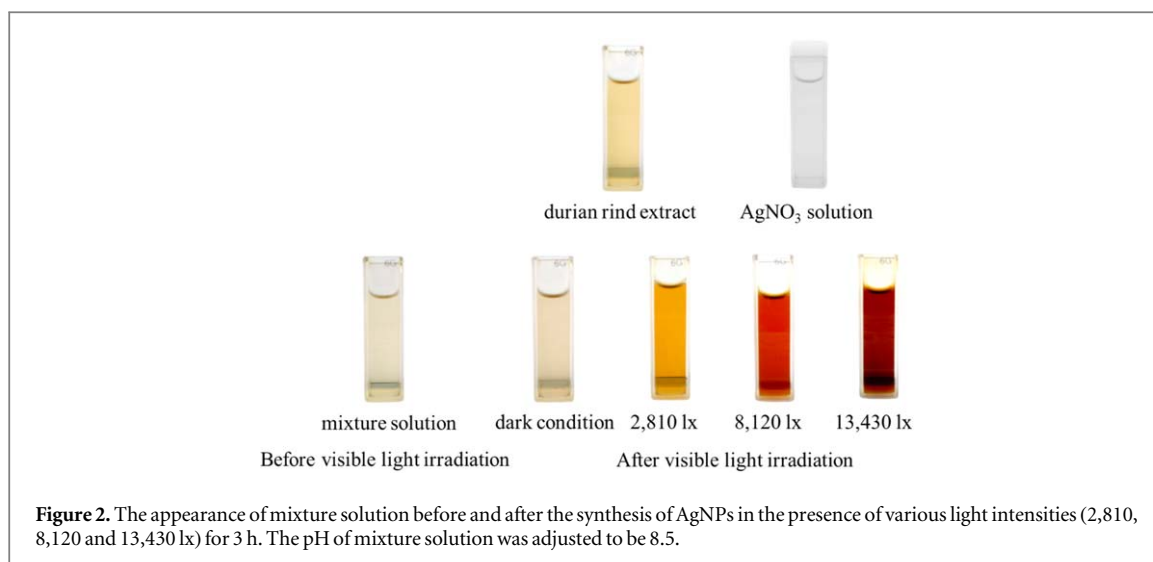


Figure 2. The appearance of mixture solution before and after the synthesis of AgNPs in the presence of various light intensities (2,810, 8,120 and 13,430 lx) for 3 h. The pH of mixture solution was adjusted to be 8.5.

3. Results and discussion

In this work, the photo-irradiation induced synthesis of AgNPs using durian rind extract was studied. The important operational parameter including light intensity, exposure time, and pH solution were varied to investigate the spherical particle size, experimental yield and colloidal stability of AgNPs. The achieved experimental results were described below.

3.1. Effect of light intensity on the synthesis of AgNPs

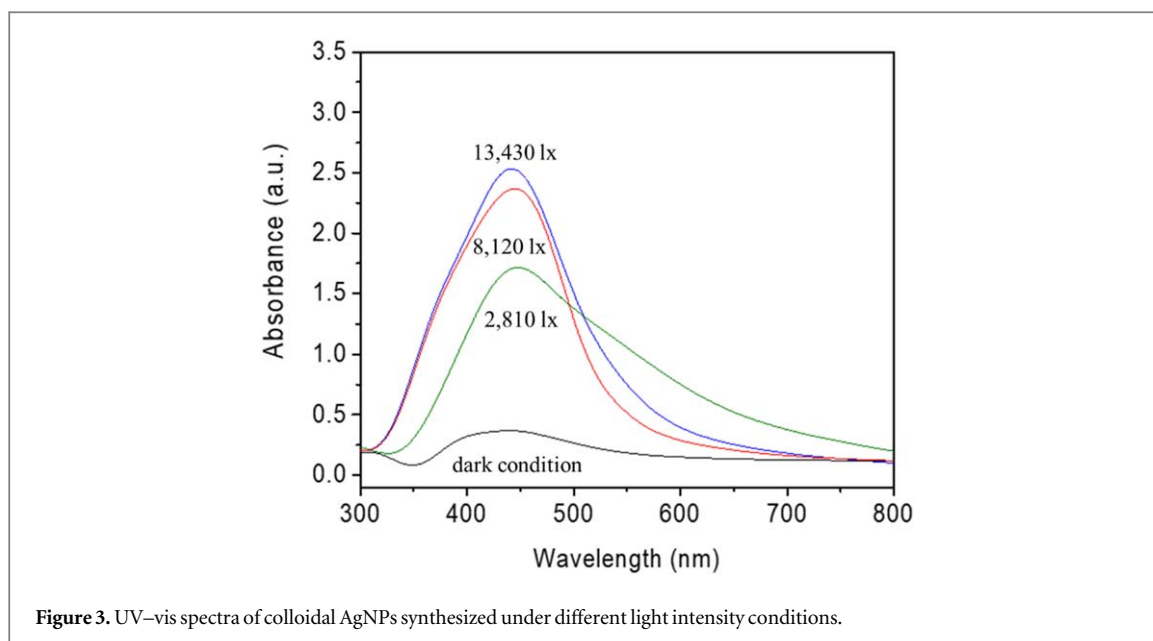
After subjecting the mixture of extract and AgNO_3 solution under the visible light for 3 h without heat treatment, the color of mixture changed from pale yellow, which was natural color of the extract, to orange-brown and became darker with increasing the light intensity as illustrated in figure 2. The appearance of these color changes arise from the collective oscillation of electrons on the surface of metal particles as a result of the interaction with an electric field component of the incident light in a phenomenon called surface plasmon resonance (SPR) [35, 48, 49]. The SPR, which is a unique optical property of nanomaterials, induces a strong absorption of the incident light leading to SPR band or absorption spectra that can be obtained using UV–vis spectrophotometer. Generally, the SPR peak of the spherical AgNPs is confined to the visible region in the range of 400–450 nm, where the wavelength of maximum absorbance (λ_{max}) and the plasmon peak intensity associate with the size and number of AgNPs [35, 50].

Figure 3 shows the UV–vis absorption spectra of the colloidal AgNPs prepared under different light intensities of 0 (dark place), 2,810, 8,120 and 13,430 lx. It was found that all spectra occupied the λ_{max} value around 428 nm, additionally, the peak intensity increased with increasing light intensity corresponding to the change in color of the reaction mixture as displayed in figure 2. Since the AgNO_3 solution was colorless and the durian rind extract showed a flat absorbance at this wavelength (data not shown). Therefore, these results confirmed that the AgNPs with spherical shape were formed and a higher number of particles was produced after continuous exposure to higher light intensity as previous found by several researchers [48, 51]. This real phenomenon proved that the reduction rate of Ag^+ to Ag^0 could be efficiently accelerated through visible light exposure. Consequently, the light intensity of 13,430 lx was selected for further experiments.

3.2. Effect of pH and exposure time on the synthesis of AgNPs

The formation process of AgNPs involves with the nucleation, growth, and aggregation stages, accordingly, the pH value of the reaction medium that considerably results in the altering charge of macromolecule plays a major role in the chemistry of the AgNPs synthesis [52–54]. Moreover, the visible light irradiation time or known as exposure time also influences the growth of AgNPs. Therefore, investigating the effects of pH and exposure time on the formation of AgNPs were done simultaneously in this part. The extract pH was adjusted from 4.5 to 12.0; for each pH value, the mixture solution was irradiated under light intensity of 13,430 lx by varying the exposure time from 5 min to 12 h.

The kinetics of AgNPs formation process at different pH values was monitored with an UV–vis spectrophotometer. From the recorded absorption spectra demonstrated in figure 4, it showed that the absorbance intensity at λ_{max} increased by the increase of exposure time and the redshift in the wavelength of the absorbance peak to the longer wavelength was also observed under the synthetic reaction at pH 4.5, 6.5, and 7.5.



This suggested that the longer exposure time enhanced reduction process of Ag^+ to Ag^0 and the particle aggregation leading to the increase of the number and size of AgNPs. Furthermore, the UV-vis spectra as shown in figure 4 could be observed that the photoreduction reaction at a pH value of greater than 4.5 occurred within 5 min after visible light exposure, however, the AgNPs formation rate increased with increasing pH equal to pH 8.5 and then the formation rate decreased. It indicated that alkaline medium provided a better appropriate condition for particle growth than acidic medium due to the increase of negatively charged hydroxide ions (OH^-), resulting in fast reduction of Ag^+ to Ag^0 and fast nucleation of silver from the reduction of Ag^+ ; while the slow rate of reduction observed in the acidic medium could be arise from electrostatic repulsion of anions presented in the reaction mixture [52, 53, 55]. The explicit evidence of the effects of pH and exposure time on the growth rate of AgNPs is shown in figure 5. To reach almost complete formation of AgNPs, there required an exposure time of 6 h, 3 h, 3 h, 5 min, and 5 min for pH 4.5, 6.5, 7.5, 8.5, and 12, respectively. The pH value of 8.5 gave the highest maximum yield of AgNPs in comparison to synthesize under other pH values (pH 4.5, 6.5, 7.5, and 12).

Additionally, from figure 4, it can be observed that the λ_{max} value for acidic condition (pH 4.5) peaked at around 451 nm and it was blue shifted toward a shorter wavelength of around 415 nm in the case of alkaline condition (pH 12). It suggested that the size of synthesized AgNPs tended to decrease when the pH value increased because fast nucleation process occurred, resulting in forming high amount of small size particles [37, 56, 57]. While at acidic pH, the nucleation rate was slow, leading to formation of large size particle with low amount. This phenomenon was also observed by another research group [58]. Compared to pH values of 8.5 and 12, there was no significant shift in the λ_{max} whereas the full width at half maximum (FWHM) of the absorbance band at pH 12 was wider than pH 8.5, indicating the wider particle size distribution. Therefore, a pH of 8.5 was selected as the optimum pH value of reaction medium.

3.3. Characterization of green synthesized AgNPs

From all above mentioned results, it can be concluded that the optimum condition for the photo-induced green synthesis of AgNPs from durian rind extract was exposure to visible light intensity of 13,430 lx for 5 min with a pH of 8.5. The as-prepared AgNPs obtained from this condition is shown in figure 6. The formation of dispersion and uniform nanoparticles was confirmed by TEM image and the corresponding narrow size distribution histogram. As illustrated in figure 6, their main morphology was spherical in shape with 11.4 nm mean size and size distribution ranging from 5 to 17 nm. Whereas, the average hydrodynamic size of AgNPs suspended in de-ionized water analyzed by dynamic light scattering (DLS) technique was 32.4 ± 1.7 nm and the polydispersity index was found to be 0.199. As can be seen that the DLS size was remarkably larger than the TEM size. This difference in size might be due to the influence of Brownian motion [7] and capping agent molecules attached on the surface moving with the AgNPs in solution [59].

The crystalline structure of synthesized AgNPs was revealed by XRD pattern in figure 7(a). It shows four sharp diffraction peaks of the face centered cubic (FCC) lattice corresponding to silver element (JCPDS no.04-0783). The peaks were observed at 38.1° , 44.2° , 64.4° and 77.4° in the 2θ range of 30° to 80° , which can be

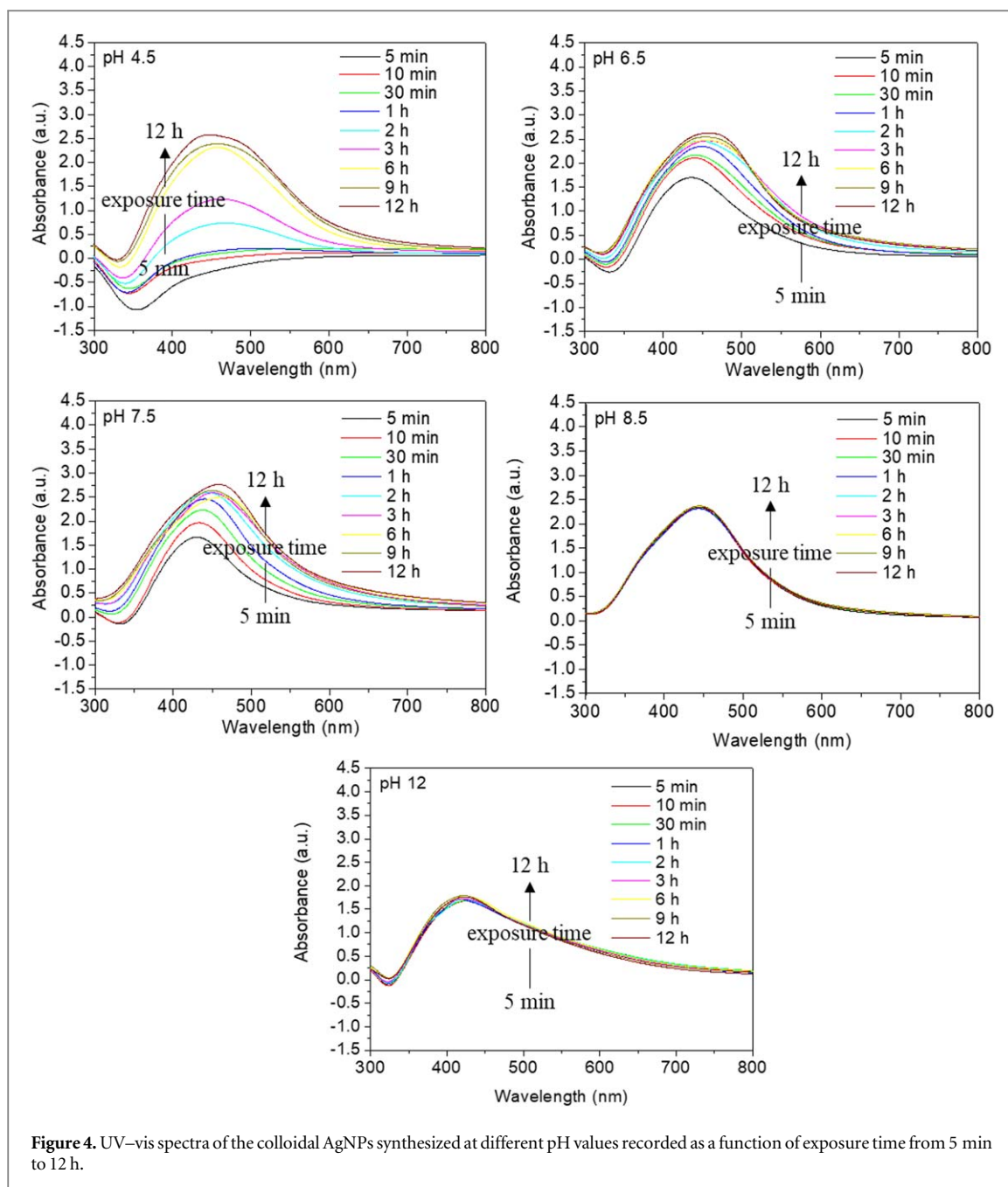


Figure 4. UV-vis spectra of the colloidal AgNPs synthesized at different pH values recorded as a function of exposure time from 5 min to 12 h.

assigned to (111), (200), (220) and (311) lattice planes of crystalline silver. Additionally, the collected EDX spectrum as shown in figure 7(b) also confirmed the presence of silver element.

The yield of collected AgNPs synthesized under the optimal condition was carried out by ICP-OES. After calculation, it was found that the high yield of approximately 99% was achieved. Their ensuring stability is of crucial importance for storage and further potential application in various fields such as antimicrobial activity, biosensors, and catalysis. Thus, the zeta potential was determined to examine the stability of obtained colloidal AgNPs. Normally, the absolute value of zeta potential higher than 30 mV indicates high stable state of colloidal systems [37, 51]. The colloidal of AgNPs produced in this work exhibited negative zeta potential with the absolute value of 53.2 ± 1.6 mV, indicating their excellent long-term dispersion stability due to a strong negative-negative electrostatic repulsion. Besides, the negative value of zeta potential reflected the presence of some bio-organic capping molecules, preventing the nanoparticles agglomeration [45]. In this realistic experiment, the suspension was stable more than six months at 4 °C in darkness (refrigerated).

3.4. Possible mechanism of biosynthesis of AgNPs

Previous researches showed the possible biomolecules responsible for reducing and capping AgNPs synthesized using durian rind extract [41, 45]. However, the exact mechanism for the synthesis of AgNPs in the presence of

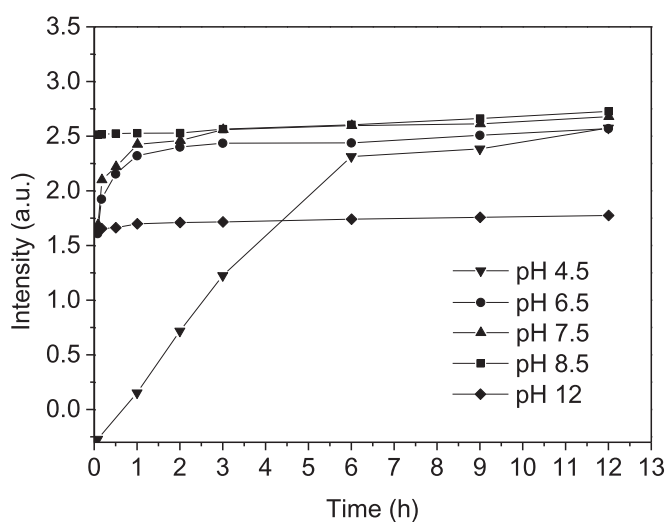


Figure 5. Evaluation of the absorbance at λ_{\max} as a function of the exposure time.

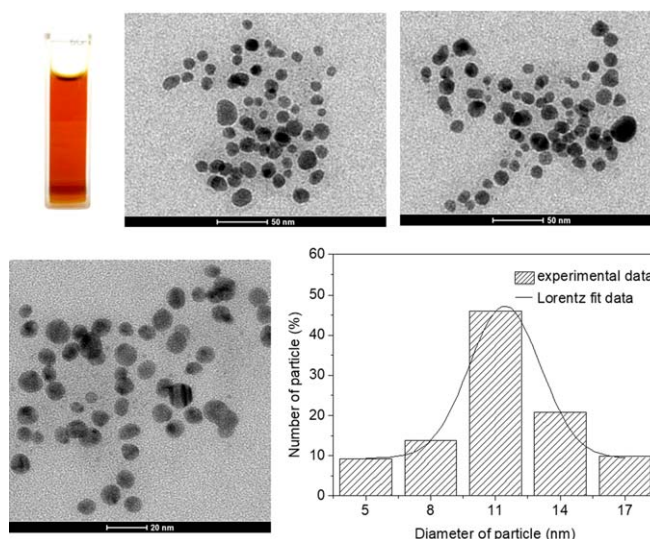


Figure 6. Digital photograph of as-prepared AgNPs, representative TEM image and the associated particle size distribution histogram of the synthesized AgNPs.

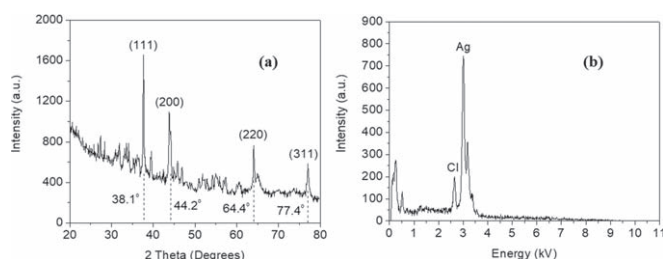
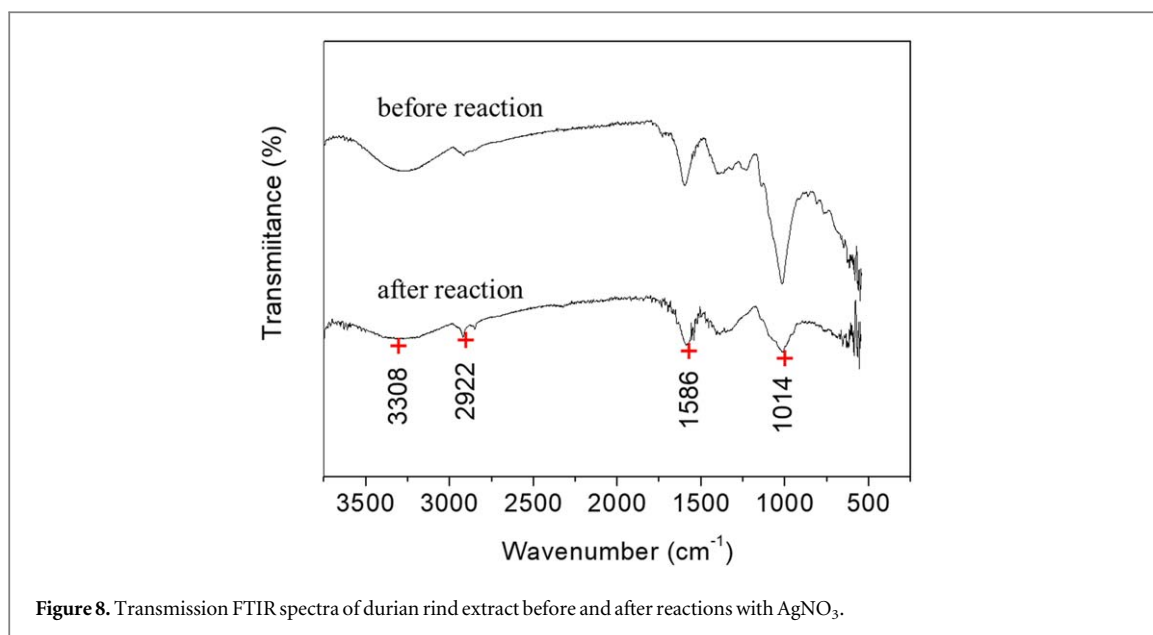


Figure 7. (a) x-ray diffraction pattern of synthesized AgNPs. (b) Representative EDS spectrum of synthesized AgNPs confirming presence of silver.

durian rind extract has not yet been empirically demonstrated. HPLC and FTIR can be valuable tools to help in understanding the specific synthesis mechanism. HPLC analysis revealed that two major sugars detected in white part of durian rind was glucose and fructose with the amount of 1.01 g/100 g and 0.93 g/100 g, respectively. In addition, the protein content of 0.09 g/100 ml was also found. The FTIR spectra of durian extract



before and after reactions with AgNO_3 obtained in this study are shown in figure 8. The main intense bands were located at around 3308 cm^{-1} from OH-stretching of phenol and alcohol, 2922 to 2851 cm^{-1} from C–H stretching, 1586 cm^{-1} from N–H deformation vibrations in the amide linkage of protein, and 1014 cm^{-1} from C–OH stretching alcohols or C-stretching ether group [25, 45, 51, 53]. However, a decrease in transmission intensity of all FTIR peaks after complete reaction was clearly observed.

The presence of these compositions and functional groups suggested that the extract exhibited both the reducing as well as capping properties. A large number of hydroxyl groups of flavonoids, the other phenolic compounds, and glucose possibly involved the reducing Ag^+ to Ag atoms that aggregated in Ag clusters and AgNPs. Whereas fructose itself could not play the role as a reducing agent, it was converted into glucose by a tautomerism [38]. The presence of proteins in the durian rind extract might be responsible for the preventing particles from adhering and agglomerating, leading negative zeta potential of AgNPs due to capping with negative charged proteins [51].

4. Conclusions

In summary, the present work clearly demonstrated that the white part of durian rind extract was successfully used for photo-induced rapid green synthesis of AgNPs with small size, narrow particle size distribution, and remarkable excellent stability. The visible light intensity, reaction time, and pH value were proved to be crucial parameters in controlling the shape, size, formation rate, and concentration of the produced AgNPs. Due to very small size green AgNPs around 10 nm obtained under optimum reaction parameters, it could exhibit strong antibacterial activity. Therefore, this proposed synthesis method is a step-by-step and repeatable procedure for developing AgNPs, which could be applied in various fields such as antimicrobial activity, biosensors, and catalysis. Additionally, the present synthesis method is an efficient alternative approach for sustainable waste management by the use of abundant agricultural waste for the manufacturing of nanoparticles.

Acknowledgments

The authors would like to thank Science Achievement Scholarship of Thailand and Faculty of Science, King Mongkut's University of Technology Thonburi for financial support.

ORCID iDs

Fueangfahkan Chutrakulwong  <https://orcid.org/0000-0001-6075-8743>

References

- [1] de Jesús Ruíz-Baltazar Á, Reyes-López S Y, Larrañaga D, Estévez M and Pérez R 2017 Green synthesis of silver nanoparticles using a *Melissa officinalis* leaf extract with antibacterial properties *Res. Phys.* **7** 2639–43
- [2] Singh A K, Tiwari R, Kumar V, Singh P, Riyazat Khadim S K, Tiwari A, Srivastava V, Hasan S H and Asthana R K 2017 Photo-induced biosynthesis of silver nanoparticles from aqueous extract of *Dunaliella salina* and their anticancer potential *J. Photochem. Photobiol. B* **166** 202–11
- [3] Ravichandran V, Vasanthib S, Shalinic S, Ali Shahd S A, Tripathy M and Paliwala N 2019 Green synthesis, characterization, antibacterial, antioxidant and photocatalytic activity of *Parkia speciosa* leaves extract mediated silver nanoparticles *Res. Phys.* **15** 1–8
- [4] Rittichai T and Pimpan V 2019 Ammonia sensing of silver nanoparticles synthesized using tannic acid combined with UV radiation: effect of UV exposure time *J. King Saud Univ. Sci.* **31** 277–84
- [5] Loiseau A, Asila V, Boitel-Aullen G, Lam M, Salmain M and Boujday S 2019 Silver-based plasmonic nanoparticles for and their use in biosensing *Biosensors (Basel)*. **9** 1–39
- [6] Fang H, Zhang X, Zhang S J, Liu L, Zhao Y M and Xu H J 2015 Ultrasensitive and quantitative detection of paraquat on fruits skins via surface-enhanced Raman spectroscopy *Sens. Act. B* **213** 452–6
- [7] Zhang X F, Liu Z G, Shen W and Gurunathan S 2016 Silver nanoparticles: synthesis, characterization, properties, applications, and therapeutic approaches *Int. J. Mol. Sci.* **17** 1–34
- [8] Lee S H and Jun B H 2019 Silver nanoparticles: synthesis and application for nanomedicine *Int. J. Mol. Sci.* **20** 1–23
- [9] Zhang Z, Shen W, Xue J, Liu Y, Liu Y, Yan P, Liu J and Tang J 2018 Recent advances in synthetic methods and applications of silver nanostructures *Nanoscale Res. Lett.* **13** 1–18
- [10] Huang N M, Lim H N, Radiman S, Khiew P S, Chiu W S, Hashim R and Chia C H 2010 Sucrose ester micellar-mediated synthesis of Ag nanoparticles and the antibacterial properties *Colloids Surf. A* **353** 69–76
- [11] Darroudi M, Ahmad M B, Abdullah A H, Ibrahim N A and Shamel K 2010 Effect of accelerator in green synthesis of silver nanoparticles *Int. J. Mol. Sci.* **11** 3898–905
- [12] Darroudi M, Zak A K, Muhamad M R, Huang N M and Hakimi M 2012 Green synthesis of colloidal silver nanoparticles by sonochemical method *Mater. Lett.* **66** 117–20
- [13] Kumar B, Smita K, Cumbal L, Debut A and Pathak R N 2014 Sonochemical synthesis of silver nanoparticles using starch: a comparison *Bioinorg. Chem. Appl.* **2014** 1–8
- [14] Seku K, Gangapuram B R, Pejjai B, Kadimpati K K and Golla N 2018 Microwave-assisted synthesis of silver nanoparticles and their application in catalytic, antibacterial and antioxidant activities *J. Nanostruct. Chem.* **8** 179–88
- [15] Zhao Z, Chamele N, Kozicki M, Yao Y and Wang C 2019 Photochemical synthesis of dendritic silver nanoparticles for anti-counterfeiting *J. Mater. Chem. C* **7** 6099–104
- [16] Spadaro D, Barletta E, Barreca F, Currò G and Neri F 2010 Synthesis of PMA stabilized silver nanoparticles by chemical reduction process under a two-step UV irradiation *Appl. Surf. Sci.* **256** 3812–6
- [17] Rahman A, Kumar S, Bafana A, Lin J, Dahoumane S A and Jeffryes C 2019 A mechanistic view of the light-induced synthesis of silver nanoparticles using extracellular polymeric substances of *Chlamydomonas reinhardtii* *Molecules*. **24** 1–19
- [18] Behravan M, Hossein Panahi A, Naghizadeh A, Ziaee M, Mahdavi R and Mirzapour A 2019 Facile green synthesis of silver nanoparticles using *Berberis vulgaris* leaf and root aqueous extract and its antibacterial activity *Int. J. Biol. Macromol.* **124** 148–54
- [19] Devi M, Devi S, Sharma V, Rana N, Bhatia R K and Bhatt A K 2020 Green synthesis of silver nanoparticles using methanolic fruit extract of *Aegle marmelos* and their antimicrobial potential against human bacterial pathogens *J. Tradit. Complement. Med.* **10** 158–65
- [20] Dong C, Cao C, Zhang X, Zhan Y, Wang X, Yang X, Zhou K, Xiao X and Yuan B 2017 Wolfberry fruit (*Lycium barbarum*) extract mediated novel route for the green synthesis of silver nanoparticles *Optik* **130** 162–70
- [21] Bindhu M R, Umadevi M, Esmail G A, Al-Dhabi N A and Arasu M V 2020 Green synthesis and characterization of silver nanoparticles from *Moringa oleifera* flower and assessment of antimicrobial and sensing properties *J. Photochem. Photobiol. B* **205** 1–28
- [22] Vasileva P, Donkova B, Karadjova I and Dushkin C 2011 Synthesis of starch-stabilized silver nanoparticles and their application as a surface plasmon resonance-based sensor of hydrogen peroxide *Colloids Surf. A. Physicochem. Eng. Asp.* **382** 203–10
- [23] Kalaiselvi D, Mohankumar A, Shanmugam G, Nivitha S and Sundararaj P 2019 Green synthesis of silver nanoparticles using latex extract of *Euphorbia tirucalli*: a novel approach for the management of root knot nematode, *Meloidogyne incognita* *Crop Protect.* **117** 108–14
- [24] Chandru M, Logesh R, Rani S K, Ahmed N and Vasimalai N 2019 One-pot green route synthesis of silver nanoparticles from jack fruit seeds and their antibacterial activities with *Escherichia coli* and *Salmonella* bacteria *Biocat. Agri. Biotech.* **20** 1–7
- [25] Philip D 2010 Honey mediated green synthesis of silver nanoparticles *Spectrochim. Acta. A. Mol. Biomol. Spectrosc.* **75** 1078–81
- [26] Edison T N J I, Atchudan R, Karthik N, Balaji J, Xiong D and Lee Y R 2020 Catalytic degradation of organic dyes using green synthesized N-doped carbon supported silver nanoparticles *Fuel*. **280** 1–7
- [27] Edison T N J I, Lee Y R and Sethuraman M G 2016 Green synthesis of silver nanoparticles using *Terminalia cuneata* and its catalytic action in reduction of direct yellow-12 dye *Spectrochim. Acta A* **161** 122–9
- [28] Vitisvorakarn T, Songtanak S, Pupang S and Noppapart W 2018 Agricultural statistics of Thailand *Bureau of Agricultural Economic Research*. **38** 64–6 <http://www.oae.go.th/>
- [29] Isvilanonda S 2019 Durian global market report *Agricultural Research Development Agency*. **11** 3 <https://www.trf.or.th/component/attachments/download/4827>
- [30] Wai W W, Alkarkhi A F M and Easa A M 2010 Comparing biosorbent ability of modified citrus and durian rind pectin *Carbohydr. Polym.* **79** 584–9
- [31] Wai W W, Alkarkhi A F M and Easa A M 2010 Effect of extraction conditions on yield and degree of esterification of durian rind pectin: An experimental design *Food Bioprod. Process.* **88** 209–14
- [32] Kunarto B and Sani E Y 2018 Antioxidant activity of extract from ultrasonic-assisted extraction of durian peels *J. Appl. Food Technol.* **5** 25–9
- [33] Hokputsa S, Gerddit W, Pongsamart S, Inngjerdigen K, Heinze T, Koschella A, Harding S E and Paulsen B S 2004 Water-soluble polysaccharides with pharmaceutical importance from durian rinds (*Durio zibethinus* Murr.): isolation, fractionation, characterisation and bioactivity *Carbohydr. Polym.* **56** 471–81
- [34] Pholdaeng K and Pongsamart S 2010 Studies on the immunomodulatory effect of polysaccharide gel extracted from *Durio zibethinus* in *Penaeus monodon* shrimp against *Vibrio harveyi* and WSSV *Fish Shellfish Immunol.* **28** 555–61
- [35] Zuurro A, Iannone A, Natali S and Lavecchia R 2019 Green synthesis of silver nanoparticles using bilberry and red current waste extracts *Processes*. **7** 1–11

- [36] Manno D, Filippo E, Di Giulio M and Serra A 2008 Synthesis and characterization of starch-stabilized Ag nanostructures for sensors applications *J. Non-Cryst. Solids* **354** 5515–20
- [37] Filip G A et al 2019 UV-light mediated green synthesis of silver and gold nanoparticles using Cornelian cherry fruit extract and their comparative effects in experimental inflammation *J. Photochem. Photobiol. B* **191** 26–37
- [38] Ullah N, Li D, Xiao-dong C, Yasin S, Umair M, Eede S V and Wei Q 2015 Photo-irradiation based biosynthesis of silver nanoparticles by using an ever green shrub and its antibacterial study *Dig. J. Nanomater. Biostruct.* **10** 95–105
- [39] Ahmed Q, Gupta N, Kumar A and Nimesh S 2017 Antibacterial efficacy of silver nanoparticles synthesized employing Terminalia arjuna bark extract *Artif. Cells Nanomed. Biotechnol.* **45** 1192–200
- [40] Chen Y, Sun W, Qu D, Zhou J and Liu C 2014 Synthesis and *in vitro* antineoplastic evaluation of silver nanoparticles mediated by Agrimoniae herba extract *Int. J. Nanomed.* **9** 1871–82
- [41] Chutrakulwong F and Thamaphat K 2014 Durian peeling extract mediated green synthesis of silver nanoparticles *Adv. Mater. Res.* **875–877** 18–22
- [42] Kaviya S, Santhanalakshmi J, Viswanathan B, Muthumary J and Srinivasan K 2011 Biosynthesis of silver nanoparticles using citrus sinensis peel extract and its antibacterial activity *Spectrochim. Acta. A. Mol. Biomol. Spectrosc.* **79** 594–8
- [43] Bastos-Arrieta J, Florido A, Pérez-Ráfols C, Serrano N, Fiol N, Poch J and Villaescusa I 2018 Green synthesis of Ag nanoparticles using grape stalk waste extract for the modification of screen-printed electrodes *Nanomater.* **8** 1–14
- [44] Bankar A, Joshi B, Kumar A R and Zinjarde S 2010 Banana peel extract mediated novel route for the synthesis of silver nanoparticles *Colloids Surf. A. Physicochem. Eng. Asp.* **368** 58–63
- [45] Sumitha S, Vasanthi S, Shalini S, Chinni S V, Gopinath S C B, Kathiresan S, Anbu P and Ravichandran V 2019 Durio zibethinus rind extract mediated green synthesis of silver nanoparticles: Characterization and biomedical applications *Phcog. Net.* **15** 52–8
- [46] San H N, Lu G, Shu D and Yu T X 2020 Mechanical properties and energy absorption characteristics of tropical fruit durian (Durio zibethinus) *J. Mech. Behav. Biomed. Mater.* **104** 1–13
- [47] Horwitz W and Latimer G W 2005 Official methods of analysis of AOAC International 18 edition AOAC International Gaithersburg Maryland 8-106
- [48] Mokhtari N, Daneshpajouh S, Seyedbagheri S, Atashdehghan R, Abdi K, Sarkar S, Minaian S, Shahverdi H R and Shahverdi A R 2009 Biological synthesis of very small silver nanoparticles by culture supernatant of Klebsiella pneumonia: the effects of visible-light irradiation and the liquid mixing process *Mater. Res. Bull.* **44** 1415–21
- [49] Rastogi L and Arunachalam J 2011 Sunlight based irradiation strategy for rapid green synthesis of highly stable silver nanoparticles using aqueous garlic (Allium sativum) extract and their antibacterial potential *Mater. Chem. Phys.* **129** 558–63
- [50] Challa K 2019 Chemistry of nanomaterialsvolume 1: Metallic nanomaterials (Part B)De Gruyter Harvard University Cambridge USA 1-339
- [51] Wei W, Luo M, Li W, Yang L, Liang X, Xu L, Kong P and Liu H 2012 Synthesis of silver nanoparticles by solar irradiation of cell-free Bacillus amyloliquefaciens extracts and AgNO₃ *Bioresour. Technol.* **103** 273–8
- [52] Andries M, Pricop D, Oprica L, Creanga D-E and Iacomì F 2016 The effect of visible light on gold nanoparticles and some bioeffects on environmental fungi *Int. J. Pharm.* **505** 255–61
- [53] Traiwatcharanon P, Timsorn K and Wongchoosuk C 2017 Flexible room-temperature resistive humidity sensor based on silver nanoparticles *Mater. Res. Express* **4** 1–10
- [54] Thanh N T K, Maclean N and Mahiddine S 2014 Mechanisms of nucleation and growth of nanoparticles in solution *Chem. Rev.* **114** 7610–30
- [55] Edison T J I and Sethuraman M G 2012 Instant green synthesis of silver nanoparticles using Terminalia chebula fruit extract and evaluation of their catalytic activity on reduction of methylene blue *Process Biochem.* **47** 1351–7
- [56] Kshirsagar P, Sangaru S S, Malvindi M A, Martiradonna L, Cingolani R and Pompa P P 2011 Synthesis of highly stable silver nanoparticles by photoreduction and their size fractionation by phase transfer method *Colloids Surf. A. Physicochem. Eng. Asp.* **392** 264–70
- [57] Edison T N J I, Atchudan R, Sethuraman M G and Lee Y R 2016 Reductive-degradation of carcinogenic azo dyes using Anacardium occidentale testa derived silver nanoparticles *J. Photochem. Photobiol. B, Biol.* **162** 604–10
- [58] Chitra K and Annadurai G 2014 Antibacterial activity of pH- dependent biosynthesized silver nanoparticles against clinical pathogen *Biomed Res. Int.* **2014** 1–6
- [59] Erjaee H, Rajaian H and Nazifi S 2017 Synthesis and characterization of novel silver nanoparticles using Chamaemelum nobile extract for antibacterial application *Adv. Nat. Sci.: Nanosci. Nanotechnol.* **8** 1–9